doi:10.1016/j.jmb.2010.07.031 J. Mol. Biol. (2010) 402, 241–258

JMB

Available online at www.sciencedirect.com

ScienceDirect

ELSEVIER

Residue-Resolved Stability of Full-Consensus Ankyrin Repeat Proteins Probed by NMR

Svava K. Wetzel[1,2]†, Christina Ewald[2]†, Giovanni Settanni[3], Simon Jurt[2], Andreas Plückthun[1]* and Oliver Zerbe[2]*

[1]*Institute of Biochemistry, University of Zürich, CH-8057 Zürich, Switzerland*

[2]*Institute of Organic Chemistry, University of Zürich, CH-8057 Zürich, Switzerland*

[3]*MRC Centre for Protein Engineering, Cambridge CB2 0QH, UK*

Received 27 April 2010; received in revised form 10 July 2010; accepted 15 July 2010
Available online
July 21 2010

We investigated the stability determinants and the unfolding characteristics of full-consensus designed ankyrin repeat proteins (DARPins) by NMR. Despite the repeating sequence motifs, the resonances could be fully assigned using $^{2}H,^{15}N,^{13}C$ triple-labeled proteins. To remove further ambiguities, we attached paramagnetic spin labels to either end of these elongated proteins, which attenuate the resonances of the spatially closest residues. Deuterium exchange experiments of DARPins with two and three internal repeats between N- and C-terminal capping repeats (NI_2C, NI_3C) and NI_3C_Mut5, where the C-cap had been reengineered, indicate that the stability of the full-consensus ankyrin repeat proteins is strongly dependent on the coupling between repeats, as the stabilized cap decreases the exchange rate throughout the whole protein. Some amide protons require more than a year to exchange at 37 °C, highlighting the extraordinary stability of the proteins. Denaturant-induced unfolding, followed by deuterium exchange, chemical shift change, and heteronuclear nuclear Overhauser effects, is consistent with an Ising-type description of equilibrium folding for NI_3C_Mut5, while for native-state deuterium exchange, we postulate local fluctuations to dominate exchange as unfolding events are too slow in these very stable proteins. The location of extraordinarily slowly exchanging protons indicates a very stable core structure in the DARPins that combines hydrophobic shielding with favorable electrostatic interactions. These investigations help the understanding of repeat protein architecture and the further design of DARPins for biomedical applications where high stability is required.

Edited by K. Kuwajima

Keywords: NMR; folding; hydrogen exchange; repeat proteins; Ising model

Introduction

Repeat proteins are built of repeating structural units of typically 25–45 amino acids that stack together to build a folded domain.[1,2] Among the most common types of repeat motifs are the ankyrin repeat (AR), armadillo repeat, leucine-rich repeat, and tetratricopeptide repeat.[3]

The repeat protein architecture relies on stabilizing and structure-determining interactions formed within a repeat and between the neighboring repeats and contains no interactions between residues very far apart in the protein sequence. This modular nature of repeat proteins makes them

*Corresponding authors. E-mail addresses: plueckthun@bioc.uzh.ch; oliver.zerbe@oci.uzh.ch.

† S.K.W. and C.E. contributed equally to this work.

Abbreviations used: DARPin, designed ankyrin repeat protein; AR, ankyrin repeat; MD, molecular dynamics; H/D, hydrogen/deuterium; MEXICO, measurement of fast proton exchange rates in isotopically labeled compounds; PRE, paramagnetic relaxation enhancement; HSQC, heteronuclear single quantum coherence; NOE, nuclear Overhauser enhancement; MTSL, 1-oxyl-2,2,5,5-tetramethyl-Δ3-pyrroline-3-methyl)mercaptyl; MalNEt, *N*-ethyl-maleimide; PF, protection factor.

fundamentally different from globular proteins and thus interesting for testing experimental and theoretical views that have emerged from the study of globular proteins.

The AR is a 33-residue motif consisting of a β-turn, followed by two antiparallel α-helices and a loop reaching towards the turn of the next repeat.[4] A library of designed ankyrin repeat proteins (DARPins)[5] has been created as a source of very robust specific binding proteins for many applications in biomedicine and biochemical research. It has thus been interesting both from a fundamental and an applied perspective to understand the stability determinants of these proteins. The library contains internal repeats with randomized residues flanked by an N- and a C-terminal capping repeat.[6] The capping repeats are essential to allow the folding of these proteins within the cell,[7] and these proteins can be expressed in soluble form to very high levels.

To systematically investigate the stability determinants, we have previously designed a full-consensus AR as an idealized example for studying AR protein folding and constructed DARPins of variable length, built up by combining the N- and C-capping module (N, C) with internal identical repeats of varying number (I_1 to I_6).[8] By a systematic study of these proteins, we found an increase of stability with length, up to the point that the proteins became resistant to boiling and saturated GdmCl solutions.[8]

We have previously investigated three of our designed proteins, NI_1C, NI_2C, and NI_3C, not only by equilibrium but also by kinetic unfolding and refolding analysis, and found that all three proteins display a complex folding mechanism. While they all revealed at least a three-state mechanism in kinetic experiments, NI_3C demonstrated a stable intermediate state that is also detected in equilibrium CD measurements.[8] We suggested a possible structure of this intermediate, where the N-terminal capping repeat and all three internal full-consensus repeats are still folded, while the C-terminal capping repeat is unfolded.[7]

Combining molecular dynamics (MD) simulations and experiments,[7] we deduced that the C-terminal capping repeat, taken from a natural AR protein,[6] was the weakest link and designed improved C-caps with much higher stability.[7] From GdmCl equilibrium unfolding experiments, these new capping repeats appear to stabilize the whole protein, as the main transition is shifted to even higher GdmCl concentrations.

We wished to now obtain more detailed information of the stability determinants of these extraordinarily denaturation-resistant repeat proteins and of the structure of their intermediates and therefore used hydrogen/deuterium (H/D) exchange (HX) observed through 2D ^{1}H–^{15}N correlation spectroscopy.[9] The hydrogen exchange reactions of amides in the native state of proteins are the result of structural fluctuations that can be divided into three categories: (i) cooperative global unfolding (all residues), (ii) cooperative local unfolding (several residues), and (iii) non-cooperative local fluctuations of individual residues.

In order to relate the equilibrium stability of repeat proteins to the number of repeats, we used a 1D Ising-like model to describe the transitions.[8,10–12] This model could also describe the unfolding kinetics as a function of repeat number.[8] According to this model, each repeat is considered to be an independent folding unit that interacts with the neighboring repeat(s). In the case of DARPins, five parameters could describe the system: the coupling free energy J between repeats, the free energy of an isolated repeat ΔG_0, its denaturant dependence m, the free energy of an isolated capping repeat $\Delta G_0'$, and its denaturant dependence m'.[8]

In the present study, we intended to analyze the local stability of three proteins, NI_2C, NI_3C, and NI_3C, with the more stable C-cap, termed NI_3C _Mut5 (for sequences, see Fig. S1). We present an approach for deriving nearly complete backbone assignments, a non-trivial task due to the highly repetitive nature of the sequences. Amide proton exchange is measured using classical $^{1}H/^{2}H$ exchange experiments both in the absence and in the presence of denaturant. In order to capture the rates of the more rapidly exchanging residues, we additionally performed MEXICO (measurement of fast proton exchange rates in isotopically labeled compounds) experiments.[13] Taken together, we could obtain an extensive set of protection factors (PFs) along the sequence spanning 9 orders of magnitude. Furthermore, we monitored GdmCl-induced equilibrium unfolding by using ^{1}H–^{15}N heteronuclear NMR techniques. The data are discussed within the context of folding models, in particular with respect to Ising-type folding models.

Results

Backbone assignment of NI_2C, NI_3C, and NI_3C_Mut5

As none of the DARPins has been studied by NMR so far, the first step was to assign the ^{1}H,^{13}C,^{15}N resonances of NI_2C, NI_3C, and NI_3C _Mut5 using 3D triple-resonance NMR experiments and paramagnetic relaxation enhancement (PRE) spin labels. Signal dispersion was very good despite the α-helical fold of the proteins and the presence of identical sequence fragments (Fig. 1 and Figs. S2–S4), and linewidths indicate that all proteins are monomeric species. The [^{15}N,^{1}H]-heteronuclear single quantum coherence (HSQC) spectra of NI_2C

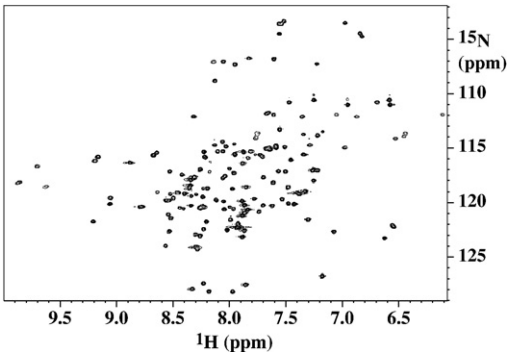

Fig. 1. [^{15}N,^{1}H]-HSQC spectrum (700 MHz) of 1.5 mM ^{15}N,^{13}C,^{2}H-labeled NI_3C_Mut5 in 50 mM phosphate and 150 mM NaCl, pH 7.4, at 310 K. For spectra of NI_2C, NI_3C, and assignments, see Supplementary Material.

and NI_3C with the original C-cap display peaks of a second, much more flexible conformation at the C terminus, which is absent in NI_3C_Mut5 (*vide infra*). Peak volume ratios of the predominant conformation to this second conformation are 2–3.5 in the case of NI_2C and 1–2.7 in the case of NI_3C. Due to differences in T_2 relaxation times of residues in the folded *versus* the unfolded conformation, these ratios cannot be reliably translated into population ratios, as the unfolded population would be overemphasized. The occurrence of a second minor species with the last five C-terminal residues unfolded, probably in equilibrium with the native species, is consistent with the previously observed more facile denaturation of the original C-cap.[7,8]

The full-consensus DARPins investigated here contain two or three identical internal repeats. Due to the near-identical structure of the individual repeats, residues at the corresponding position in different repeats possess very similar chemical shifts. However, the fact that in almost all cases peaks were individually resolved in the [^{15}N,^{1}H]-HSQC spectra prompted us to exclusively use ^{2}H,^{13}C,^{15}N-labeled proteins with constant-time 3D out-and-back experiments that terminate with recording amide proton signals. Since carbon resonances of corresponding positions in the individual repeats are extremely similar, backbone assignment must take advantage of the improved resolution in the proton–nitrogen correlation map. Critically important for the assignment process was the successful use of the HN(COCA)NH experiment that directly correlates neighboring amide moieties and only requires that resonances are resolved in the ^{15}N dimension (Fig. S5). 3D HNCO and HN(CA)CO experiments were recorded and additionally utilized for assignments. Finally, the assignments were cross-validated against all 3D spectra, and assignments were only accepted when segments could be successfully traced completely in the HN(COCA)NH, HN(CA)CO, and ^{15}N-resolved nuclear Overhauser enhancement (NOE) spectroscopy spectra.

While most ambiguities could be successfully resolved using this set of experiments, significant difficulties with the backbone assignment for the internal repeats remained. For example, both NI_3C and NI_3C_Mut5 contain two identical fragments spanning the first and second internal repeats, which are flanked by proline residues. While assignments within the repeats were achieved, the resulting lack of information on the sequential connectivity of these fragments made it impossible to distinguish assignments from the individual internal repeats. These difficulties could be successfully resolved by using a nitroxyl spin label [(1-oxyl-2,2,5,5-tetramethyl-Δ3-pyrroline-3-methyl)mercaptyl (MTSL)], attached by forming a disulfide with unique cysteines, which were introduced into the N- or C-cap. MTSL coupling resulted in the reduction of peak intensities of the respective cap region and parts of the adjacent repeat. Figure 2 displays relative intensities of amide moieties for the spin-labeled mutants NI_3C_Mut5-D28C (a) and NI_3C_Mut5-D155C (b) (see Fig. S6 for corresponding data of NI_2C and NI_3C). For example, MTSL coupled to position 155 affects the C-cap and parts of the third

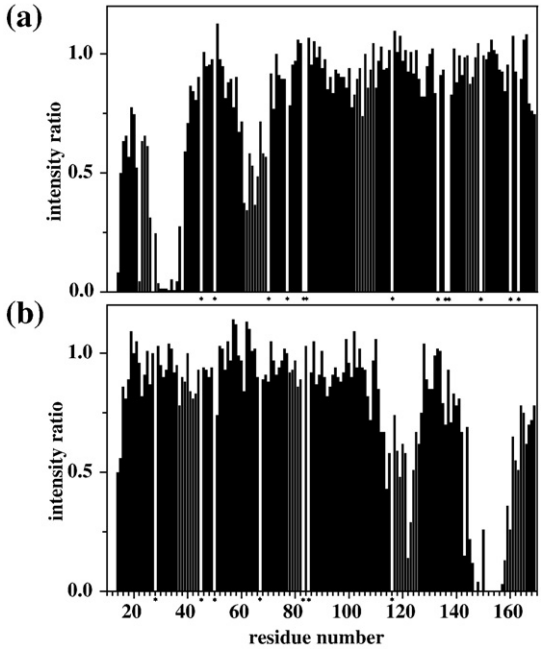

Fig. 2. PRE data of D28C (a) and D155C (b) mutants of NI_3C_Mut5. Bars represent the intensity ratios of cross-peaks (MTSL protein:reference) in the [^{15}N,^{1}H]-HSQC spectra of the MTSL-labeled Cys mutant relative to the same mutant in which the Cys residue was reduced with DTT to avoid disulfide formation and not MTSL-labeled. Values for residues that cannot be reliably integrated have been omitted and marked by a star directly below the axis.

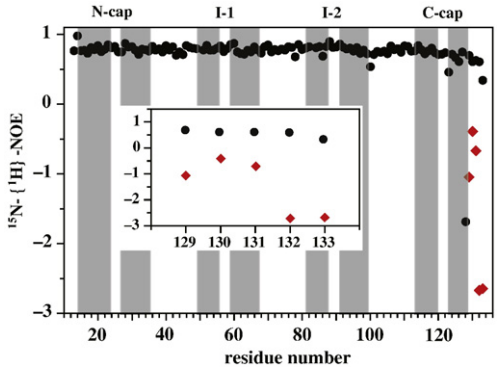

Fig. 3. ^{15}N{^{1}H}-NOE data for NI_2C recorded at 600 MHz (black circles). Data corresponding to a C-terminal minor conformation are depicted as red diamonds. The inset shows an expansion of the values at the C terminus.

repeat. The resulting pattern of distance-dependent signal attenuation in [^{15}N,^{1}H]-HSQC spectra was compared to the theoretical values computed from crystal structures and models (data not shown).

To ensure that the observed signal attenuation was not due to intermolecular effects, we coupled the respective isotopically unlabeled Cys mutant to MTSL and mixed it with the *N*-ethyl-maleimide (MalNEt)-protected ^{15}N-labeled Cys-mutant in a 1:2 (^{15}N-MalNEt:^{14}N-MTSL) ratio. In such an experiment, attenuations can only be caused by intermolecular effects. The comparison of the spectra revealed, however, that no signal reductions due to intermolecular PREs occur (see Fig. S7).

NI_2C, NI_3C, and NI_3C_Mut5 were assigned by using the procedure described above, starting from NI_2C as the smallest member of this series and exploiting this information for subsequent assignment of NI_3C and NI_3C_Mut5. The overall completeness of the backbone assignment was 99% for NI_2C, NI_3C, and NI_3C_Mut5 (see also Figs. S2–S4).

The flexibility of the second C-terminal conformation in the wild-type C-cap of NI_2C and NI_3C was verified by using heteronuclear NOE measurements. Values above 0.6 indicate well-structured regions of the protein with little internal flexibility.[14] While the ^{15}N{^{1}H}-NOE adopted values around 0.8 for most residues and positive values throughout all residues in both proteins, a second set of peaks characterized by negative ^{15}N{^{1}H}-NOEs that was assigned to the C-terminal residues was present (Fig. 3). In contrast, no such additional peaks were observed in the [^{15}N,^{1}H]-HSQC of NI_3C_Mut5.

Residue-resolved stability mapping using amide proton exchange

The full-consensus DARPins are extremely stable and thus will show ^{1}H/^{2}H exchange rates spanning many orders of magnitude. For this reason, we had to use three separate experiments to cover the full range of exchange rates: (i) To measure protons with intermediate exchange rates, we dissolved lyophilized protein in $^{2}H_2O$ and we monitored exchange by recording [^{15}N,^{1}H]-HSQC spectra at 290 K over 22 h. (ii) To record the extremely slow exchange rates of protons still present after 22 h, we incubated another sample of the protein at 310 K for several months. ^{1}H/^{2}H exchange was completed for all residues after 3 months at 310 K in the case of NI_2C and NI_3C, while for NI_3C_Mut5, even after

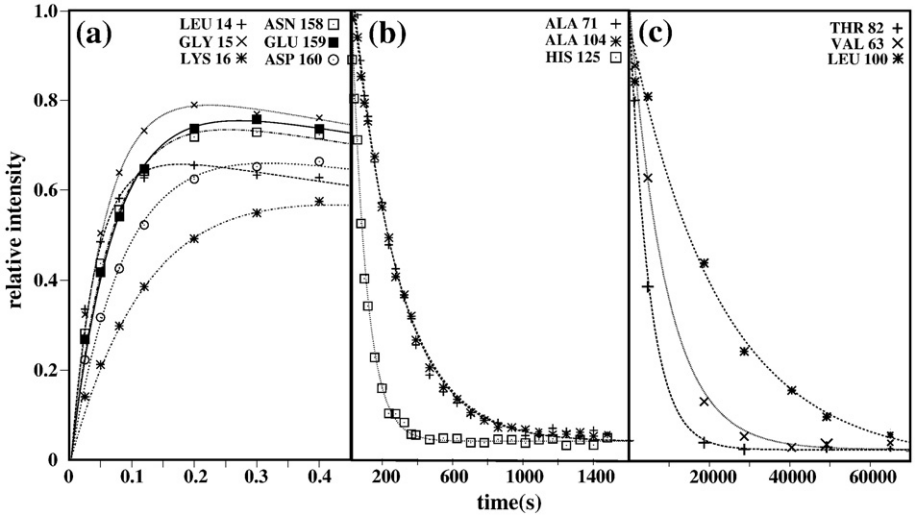

Fig. 4. Sample signal decay curves of NI_3C in the hydrogen exchange experiments. Curves correspond to data recorded using the MEXICO experiment (a), as well as classical ^{1}H/^{2}H exchange recorded at 290 K (b) and 310 K (c). Lines correspond to best fits of analytical functions [Eqs. (1) and (2)] as described in Materials and Methods.

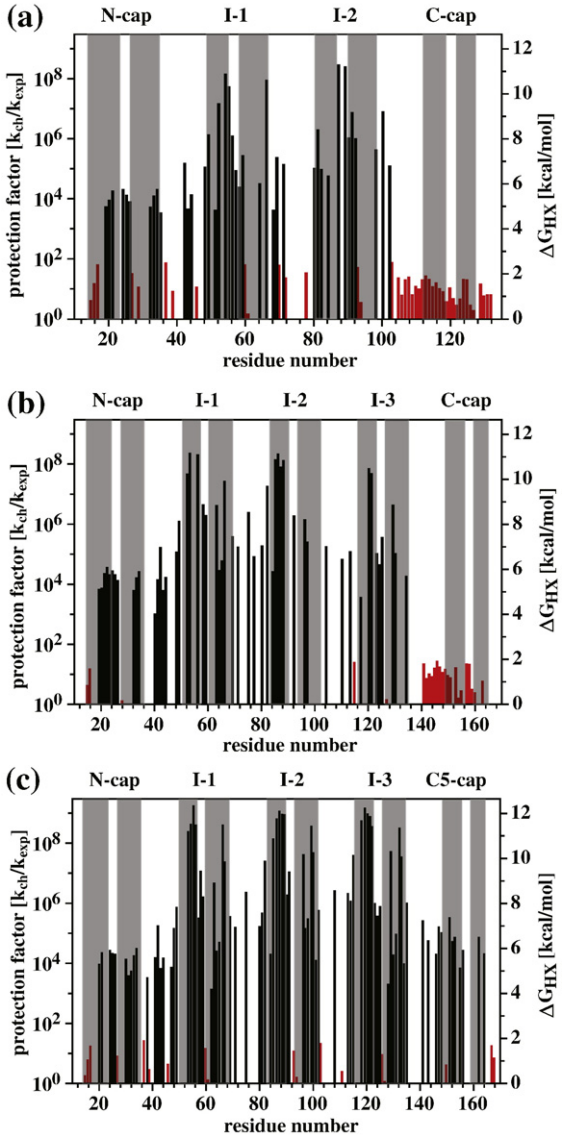

Fig. 5. Hydrogen exchange data for NI_2C, NI_3C, and NI_3C_Mut5. The free energy of exchange $\Delta G_{(HX)}$ and the PFs translated to 293 K are plotted as a function of residue number for (a) NI_2C, (b) NI_3C, and (c) NI_3C_Mut5. The secondary structure is indicated by gray background (helices). The repeat types (N-cap, C-cap, I) are indicated on top of each plot; the PFs derived from fast MEXICO rates are shown in red, while those from the $^1H/^2H$ exchange experiments are in black.

12 months, eight amide cross-peaks were still visible (*vide infra*). We therefore destabilized the protein by incubating it at 60 °C or by adding GdmCl[15] and re-measured exchange rates (*vide infra*). (iii) Finally, to also determine the rates of the fast-exchanging residues in the millisecond time range, we used the MEXICO experiment.[13] This method "bleaches" all nitrogen-attached protons and monitors re-appearance of signal intensity due to exchange with water protons. Exchange rates of 46 amides of NI_2C, 24 amides of NI_3C, and 24 amides of NI_3C_Mut5, which had disappeared before the first HSQC spectrum at 290 K, could be recorded by this method.

The rates for individual amide protons were obtained by fitting the exponential functions to corresponding cross-peak intensities as described in Materials and Methods. Examples of such fits for amides from the internal repeats as well as from the N- or C-caps of NI_3C are depicted in Fig. 4.

All rates measured at higher temperature were normalized to 293 K by using the known T dependence of $^1H/^2H$ exchange.[16] They are plotted as PFs as a function of sequence position for NI_2C, NI_3C, and NI_3C_Mut5 (Fig. 5). The PFs can then be converted into the stability difference $\Delta G_{(HX)}$ between the protected and the unprotected state of the amide (see Materials and Methods).

A few general features emerge from these investigations of DARPins (Figs. 5 and 6): (i) PFs of the capping repeats are generally lower. (ii) The PFs are higher for the N-cap than for the wild-type C-cap, while PFs of the newly designed C-cap of NI_3C_Mut5[7] are comparable to those of the N-cap. The stability of the N-cap as computed from the PF is about 6 kcal/mol in all three DARPins measured, while the stability of the wild-type C-cap is around 1.5 kcal/mol. The redesigned C-cap of NI_3C_Mut5 is about 6.5 kcal/mol and thus even slightly more stable than the N-cap. (iii) Within the internal repeats, PFs from residues in helix 1 are generally higher than those in helix 2. (iv) The PFs of NI_3C are uniform within all internal repeats and not higher for the central internal repeat of NI_3C and its mutant NI_3C_Mut5, which will be discussed in the context of expectations from an Ising model below (see Discussion). (v) Exchange rates of some of the residues from the most internal repeat of NI_3C_Mut5 are so low that a few peaks in the spectra can be followed over the time span of more than a year at 37 °C. Those residues are generally found at central positions of the helices (e.g., A55, A88, and A121 in helix 1 and L66, L99, and L132 in helix 2 of repeats 1, 2, and 3, respectively), and these PFs are close to 10^9 (Fig. 5).

Besides these general observations, specific structural features become apparent from this amide proton exchange analysis. Several residues located in long loops connecting to the next repeat of NI_3C are surprisingly well protected. For example, residues A75, A108, and Y114, whose backbone carbonyl groups are involved in hydrogen bonds with side chains of H52 and H85, display high PFs (Fig. 6). These histidine residues are part of the very conserved TPLH motifs, located at the beginning of the first helix of the internal repeats, which have previously been recognized as forming several hydrogen bonds thus connecting adjacent loops.

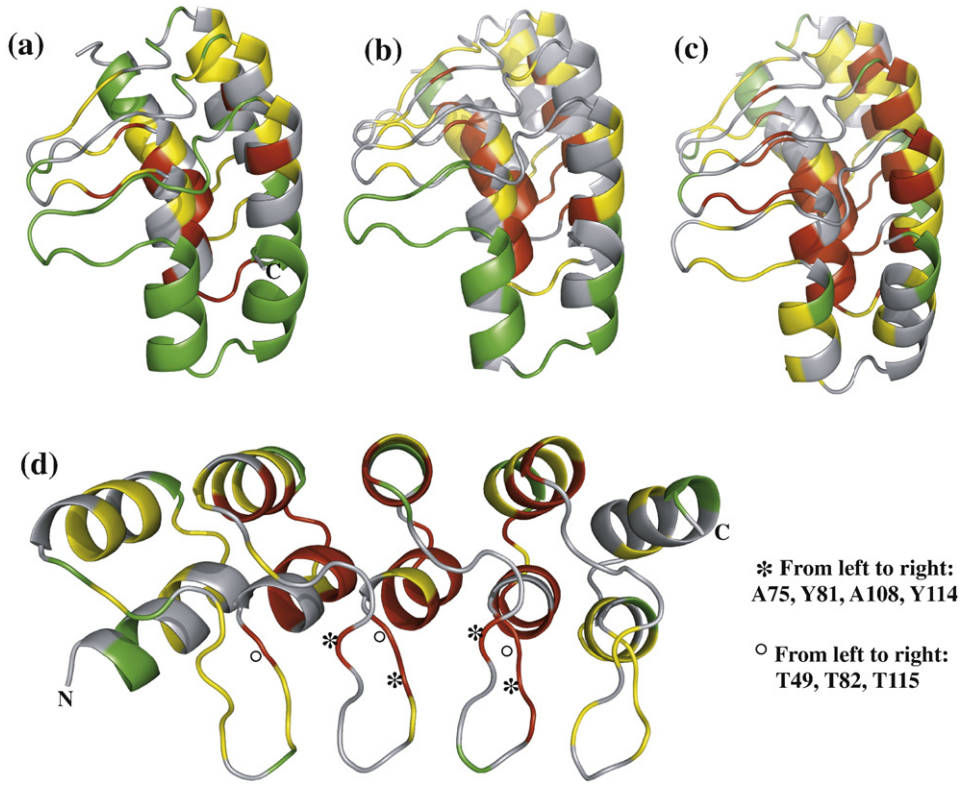

Fig. 6. Mapping of the PFs by color onto the structures of NI_2C (a), NI_3C (b), and NI_3C_Mut5 (c and d), according to the PFs of the corresponding backbone amide protons at 293 K. Residues with very low PFs ranging from 10^{-1} to 10^2 are colored green, residues with moderate PF from 10^3 to 3×10^5 are in yellow, and residues with the highest protection are in red (PF from 4.5×10^5 to 10^9). Residues for which peaks could not be integrated due to overlap are shown in gray.

Conversely, each of these loops is thereby held in place by making contacts to two histidines of TPLH motifs from adjacent repeats.[7,17]

The rates of the most slowly exchanging amides in NI_2C are characterized by PFs of about 3×10^8, corresponding to a $\Delta G_{(HX)}$ of 11 kcal/mol (Fig. 5). This value is in approximate agreement with the ΔG determined previously from denaturant-induced global unfolding (9.2±0.7 kcal/mol).[8] Most rates, however, correspond to a lower $\Delta G_{(HX)}$, indicating that exchange processes other than global unfolding, such as local unfolding and fluctuation events, must be taken into account (Fig. 5a). Denaturant-induced global unfolding curves for NI_3C and NI_3C_Mut5 were fitted assuming three- and two-state folding (19.7±4.6 and 17.9±0.7 kcal/mol, respectively). This fit, however, presents only a crude approximation because it neglects the stability difference of the C- and N-caps and assumes cooperative folding. However, even when considering the large error associated with such a fit, those data clearly demonstrate that the $\Delta G_{(HX)}$ obtained in the present work from the slowest exchanging residues (about 11 and 12.5 kcal/mol for NI_3C and NI_3C_Mut5, respectively, Fig. 5b and c) is much lower than the value from equilibrium denaturant-induced unfolding, and this difference is outside of the range of error. Therefore, we conclude that the $^1H/^2H$ exchange of the most slowly exchanging protons is not dominated by global unfolding, but contains major contributions from local unfolding and local fluctuation processes. The large difference between the PFs of the caps and the internal repeats, apparently associated to local unfolding events, emphasizes the non-cooperative nature of the folding process of these proteins, which cannot be fully captured by two- or three-state folding models.

NI_3C_Mut5 with the more stable C-cap has a denaturant-transition midpoint increased by 1.1 M GdmCl compared to NI_3C and it is characterized by a $\Delta G_{(HX)}$ for the most slowly exchanging protons of approximately 12.5 kcal/mol (Fig. 5c), which is 1.5 kcal/mol larger than that in NI_3C, demonstrating a higher overall stability of NI_3C_Mut5 throughout the internal repeats. Thus, in NI_3C_Mut5, the internal repeats display significantly higher protection than in NI_3C, although they are identical in sequence. Therefore, the redesign of the C-cap[7] has not only affected local unfolding events within the cap but also greatly improved the coupling between the C-terminal cap and the rest of the protein. This improved packing of the C-cap against

the internal repeats is also seen in the crystal structure of NI_3C_Mut5 (Kramer *et al.*, submitted). This improved coupling of the C-cap is therefore transmitted across the whole protein and apparently also retards local fluctuation events (Fig. 5c; see results from Ising model below).

Equilibrium denaturant unfolding of NI_3C and NI_3C_Mut5 analyzed by NMR

To obtain information on which regions unfold upon titration with GdmCl, we followed chemical shift changes at 20°C in [^{15}N,^{1}H]-HSQC spectra measured in the presence of increasing concentrations of GdmCl (0 to 7 M) with 200 and 300 μM ^{15}N-labeled NI_3C and NI_3C_Mut5, respectively. The buffer contained 50 mM phosphate and 150 mM NaCl at pH 7.4, as used previously in the CD and fluorescence experiments.[8]

In the first steps from 0 to 2.1 M GdmCl, several cross-peaks of the NI_3C wild-type C-cap (e.g., A141, Q142, T148–F150, G157, and A162–Q166) completely disappear or move towards the random-coil region (8.0–8.6 ppm), while new peaks appear. Representative spectra are shown in Fig. 7 and Fig. S8. In contrast, peaks from residues of the internal repeats or from the N-cap are shifted much less, and their position can still be traced over that range of GdmCl concentrations. These data clearly indicate that the C-cap of NI_3C unfolds at denaturant concentrations lower than those required for global unfolding and are thus fully consistent with our earlier proposal of this unfolding pathway.[7] In contrast, the peaks of the stabilized C-cap in NI_3C_Mut5 do not disappear, but solely shift with increasing concentration of denaturant. Signal dispersion in the HSQC spectrum of NI_3C collapses at 3.6–4 M GdmCl (Fig. S8), indicating the absence of proper side-chain packing accompanied by increased backbone flexibility. It should be noted that both collective chemical shift changes, that is, the ones involving the C-cap at 0–2.1 M GdmCl and the ones involving the other repeats at 3.6–4 M GdmCl, occur at lower GdmCl concentrations than the changes observed in the CD signature (at 3–4 M GdmCl and 5.5–6 M GdmCl, respectively).[8] This suggests that a loss of tight side-chain packing precedes the loss of secondary structure.

A more detailed analysis of the ^{15}N chemical shift changes as a function of denaturant concentration for NI_3C_Mut5 reveals that the largest changes are observed in the long loops connecting the repeats. This is particularly true not only for Asp but also for Lys residues in those parts, indicating that these residues are the primary targets of interaction with the denaturant for NI_3C_Mut5 (see Fig. S9). For protons, additional large chemical shift changes are observed at the termini of the α-helices on the face opposite to the long loops, most likely due to a slight destabilization of the helices at the ends. A similar picture emerges from the data recorded for NI_3C, but the fact that shifts cannot be monitored over

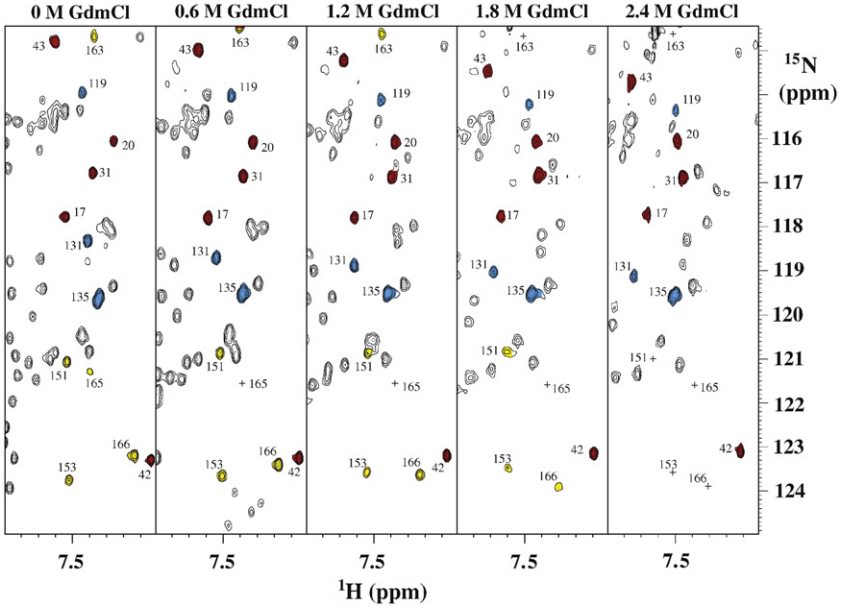

Fig. 7. Expansion from 700 MHz [^{15}N,^{1}H]-HSQC spectra of NI_3C at GdmCl concentrations of 0, 0.6, 1.2, 1.8, and 2.4 M (from left to right) at pH 7.4 and 293 K in the buffer used for the assignment. Peaks from the C-cap that disappear at elevated denaturant concentrations as well as peaks from internal repeats are annotated. Peaks from the C-cap are in yellow, those from the N-cap are in red, and those from the internal repeats are in blue.

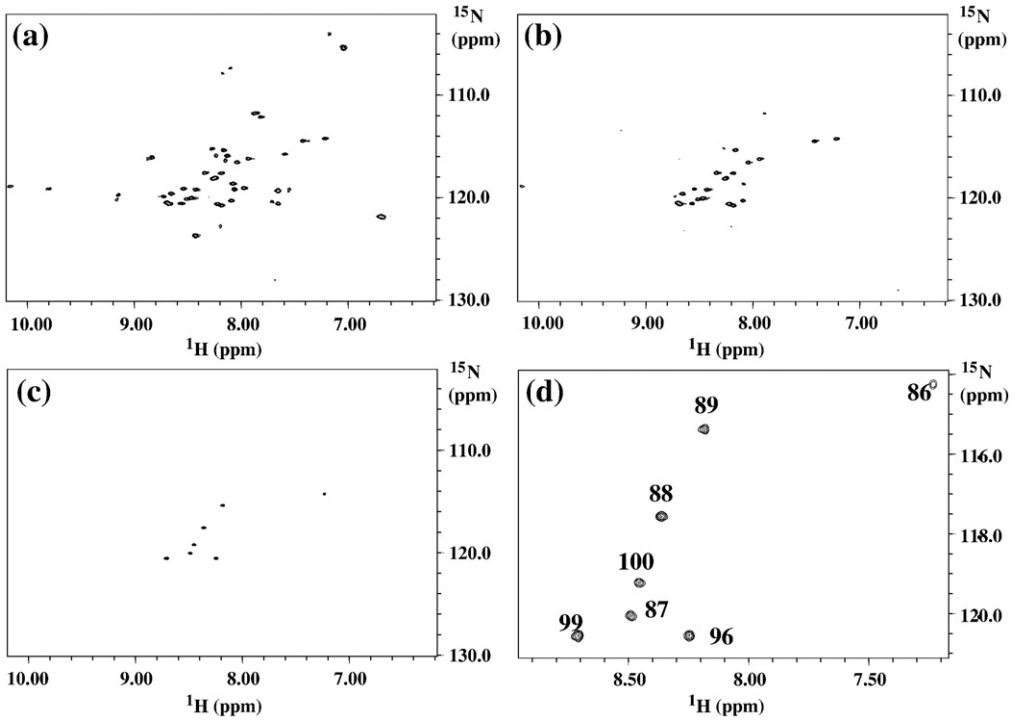

Fig. 8. [^{15}N,^{1}H]-HSQC spectra (600 MHz) of NI_3C_Mut5 in the presence of 4 M GdmCl, measured after dissolving in $^{2}H_2O$ after 0 h (a), 58 h (b), and 670 h (28 days; c and d), 310 K. The buffer used contained 50 mM phosphate and 150 mM NaCl, pH 7.4. Resonances remaining after 28 days are annotated with the corresponding residue number in the expansion shown in (d).

such a large concentration range and the additional occurrence from signals due to the intermediate complicate data analysis. Nevertheless, in both cases, the observed changes are gradual, and the ^{15}N{^{1}H}-NOE data recorded in the presence of denaturant reveal that more extensive structural changes occur only at higher concentrations of denaturant (see Fig. S10).

The ^{15}N{^{1}H}-NOEs were measured as a function of GdmCl to further investigate the destabilization of NI_3C and NI_3C_Mut5 by monitoring backbone dynamics of both proteins. At 4 M GdmCl, the ^{15}N{^{1}H}-NOEs of NI_3C are approximately 0.25–0.3 for most residues, and the amide proton exchange is very fast (*vide infra*). These observations indicate that the structure is significantly destabilized (data not shown). Considering that proton chemical shifts are sensitive to side-chain conformations while the CD signal at 222 nm is mostly sensitive to secondary structure, and taking the information from the ^{15}N{^{1}H}-NOEs into account, we propose that the changes monitored by NMR (at 3.6–4 M GdmCl) characterize reduced packing of side chains and that the changes observed by CD (at 5.5–6 M GdmCl) reflect the complete loss of secondary structure.

The spectrum of NI_3C_Mut5 still displays reasonable signal dispersion up to 5 M GdmCl (Fig. S11), while the transition identified from CD measurements is between 6.5 and 7.5 M GdmCl.[7] NI_3C_Mut5 in the absence of GdmCl is characterized by a ^{15}N{^{1}H}-NOE of 0.8, and the value is equally high both for residues of the helices and for residues of the long loops (Fig. S12c). For GdmCl concentrations up to 4 M, values still generally remain higher than 0.6 (Fig. S10), indicating that the structure remains intact and that motions are restricted to rather small fluctuations, although the decreased signal-to-noise ratio in the spectra leads to a larger scatter of the data. At 6 M GdmCl, the ^{15}N{^{1}H}-NOE adopts values about 0.25–0.3 (Fig. S10). Importantly, the data indicate that tertiary structure in NI_3C_Mut5 is present at 4 M GdmCl, and this justifies measuring amide proton exchange at 4 M denaturant in order to probe for global unfolding events.

All data obtained so far have indicated that the redesigned C-cap of NI_3C_Mut5 has a major influence on the stability of the internal repeats as well. In order to get further insight into these stability differences, we measured hydrogen exchange in the presence of deuterated GdmCl to allow observation of global unfolding events. The data for NI_3C_Mut5 clearly reveal exchange in the most central repeat to be significantly slower than that for the corresponding positions of the adjacent

repeats. After $^{1}H/^{2}H$ exchange at 310 K for approximately 1 month in the presence of 4 M GdmCl, only peaks of residues from the most central repeat are visible in the [^{15}N,^{1}H]-HSQC spectra (Fig. 8). Measurements at 3.5 M in contrast to those at 4.0 M GdmCl allowed extraction of the exchange rate constants. These rates are depicted in Fig. 9 and reveal that hydrogen exchange in GdmCl, in comparison to measurements in the absence of denaturant, is particularly accelerated in the I-1 repeat by up to 60-fold, whereas the corresponding changes for I-3 are usually smaller than 10-fold and those of I-2 are smaller still. As a result, the exchange is slowest in the central repeat. We like to point out that due to technical difficulties mainly arising from the high salt concentration, the rates cannot be extracted with the desired precision (from duplicate experiments, we estimate that errors can be up to 50% for some residues), but the relative trend is clear, and this is also obvious from the fact that only residues of the central repeat remain in spectra at later time points in 4 M GdmCl (Fig. 8d).

In addition, we have also recorded exchange spectra at 333 K (60 °C) in the absence of denaturant in order to promote global unfolding events (Fig. 9b). Exchange for I-1 is accelerated up to 20-fold and below 5-fold in I-2 and I-3. However, the differences between the repeats are small so that the central repeat is not exchanging more slowly.

Amide exchange was also measured for NI_3C at 1 and 2 M GdmCl. Measurements were complicated by the fact that many additional signals from the putative intermediate populate the spectra, leading to a decrease of signal intensity for many peaks and a large number of additional peaks that cannot be assigned. The exchange rates of the few assigned residues that can be determined reliably do not differ apparently among each other significantly, and they also do not differ from the slowly exchanging unassigned residues (see Fig. S13).

In addition, we tested pH-induced unfolding of NI_3C and NI_3C_Mut5. In these experiments, the proteins were rebuffered to pH 3.5 and [^{15}N,^{1}H]-HSQC spectra were measured. In general, the intensity of signals outside the random-coil range decrease over hours to days at 310 K, accompanied by formation of new peaks, and the protein slowly precipitates. The $^{15}N\{^{1}H\}$-NOEs mostly assume negative values indicating that the proteins unfold (data not shown). However, no quantitative data can be obtained.

Comparison to calculations based on the Ising model

An Ising model considers each repeat as an individual folding unit, characterized by an individual free energy ΔG, linearly dependent on denaturant, and stabilized by interactions with its folded neighbors, characterized by a coupling energy J.[8,11] The parameters of the Ising model describe the change in stability of the repeat as a function of environmental conditions and the magnitude of next-neighbor coupling to capture the behavior of the whole protein. In comparison to previous calculations,[8] in the present study, the model was extended to take into account the difference in stability between the N- and C-caps

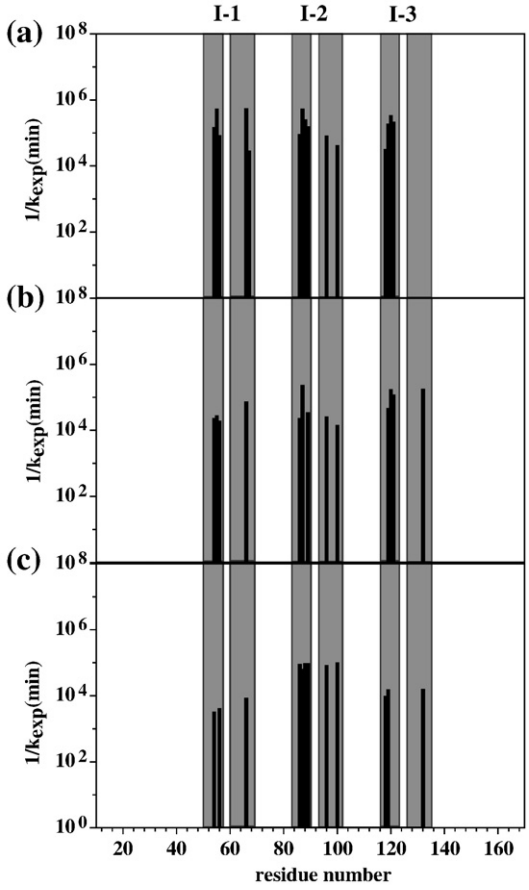

Fig. 9. PFs for selected, slowly exchanging residues of the internal repeats I-1, I-2, and I-3 of NI_3C_Mut5 measured in native buffer at 310 K (a) or 333 K (b) or in 3.5 M GdmCl at 310 K (c). [We noticed that the PFs in the measurements at 333 K or 3.5 M GdmCl surprisingly increase for many residues when compared to the measurement in buffer at 310 K. We explain it by the fact that the temperature increase or the addition of denaturant does not significantly destabilize the protein in the most stably folded regions. As a result, the only moderately accelerated exchange in those parts does not (over)compensate the large increase in the intrinsic exchange rate constant k_{ch}.] The following conversion parameters have been used for the calculations of k_{ch}: log k_A 1.5, log k_B 9.66, and log k_W −1.28 (a and b), log k_A 1.5, log k_B 10.08, and log k_W −1.825 (c),[38] where k_A, k_B, and k_W are second-order rate constants for acid, base, and water-catalyzed hydrogen exchange in poly-D,L-alanine.

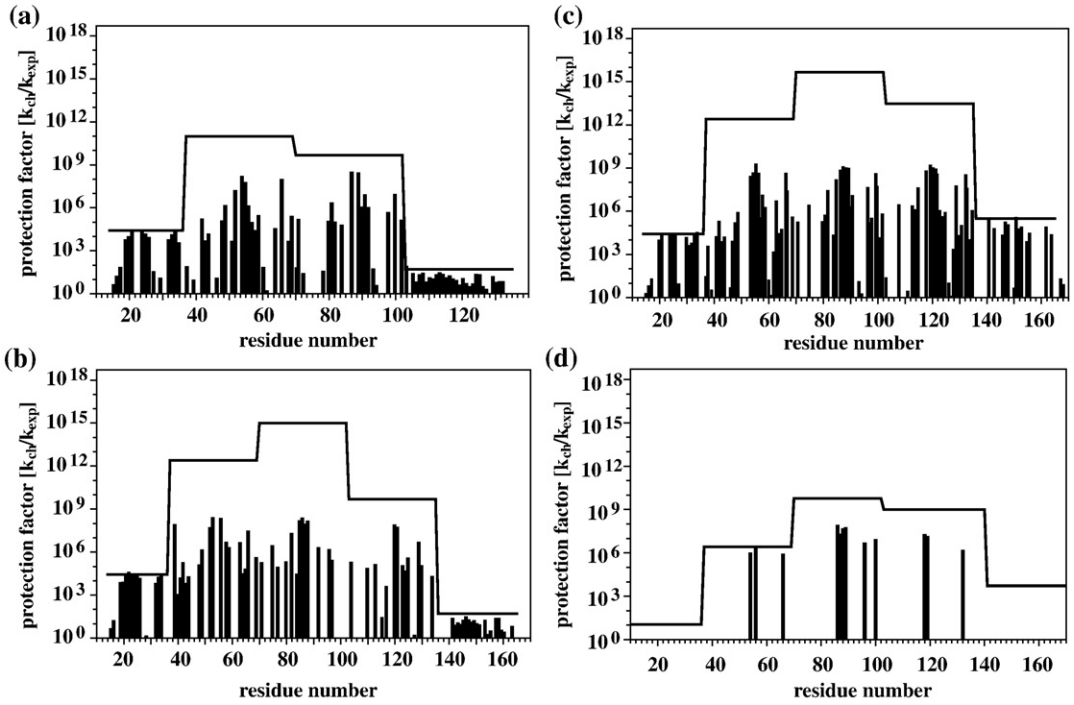

Fig. 10. Expectations of the PFs at 293 K derived from an Ising-type folding model for NI_2C (a), NI_3C (b), and NI_3C_Mut5 (c) in the absence of denaturant and NI_3C_Mut5 in the presence of 3.5 M GdmCl (d). The experimental data derived from $^1H/^2H$ exchange are shown. Note that the experimental values from $^1H/^2H$ exchange of the internal repeats have not been used in the fit, but only data from the capping repeats and unfolding data measured by CD (Fig. S14). For details, see the text.

by introducing different sets of stability parameters for the N-cap, for the original C-cap, and for the mutated C-cap (see Materials and Methods). To avoid overfitting, we globally fit the model to a large set of data, comprising the CD-monitored equilibrium unfolding of five proteins[7,8] (NI_1C, NI_2C, NI_3C, NI_1C_Mut5, and NI_3C_Mut5) and the PF values for the caps in the absence of denaturant reported in the present work. The PF values for the internal repeats have been excluded from the fit. Indeed, Ising model predictions obtained with the earlier version of the model show significantly larger PFs for the internal repeats than the experimental values (data not shown). These reasons led us to conclude that PFs of the internal repeats, despite involving extremely slow exchange rates, are seemingly the effect of local fluctuations in the native state. Exchange rates should be much slower if they were caused by complete, reversible unfolding of a single repeat, the cooperative unit of the Ising model.

If the PF of the internal repeats are excluded for the reason of local fluctuations, the model can accommodate the experimental data (see Fig. S14 for the CD data and Fig. 10 for the PF values of the caps). The extracted model parameters (see Table 1) for the repeat coupling (J), the stability of the internal repeats, and the average stability of the original caps are in good agreement with our previous computations (differences of about 1 kcal/mol). The parameters provide a quantitative measure of the difference in stability between capping repeats. In the absence of denaturant, the original C-cap is about 5 kcal/mol less stable than the mutant C-cap and almost 4 kcal/mol less stable than the N-cap.

Discussion

Repeat proteins allow testing some fundamental aspects of protein folding and stability, because of the ease with which the folded domain can be

Table 1. Thermodynamic parameters derived from the fit of the Ising model

	N-cap (N)	Internal (I)	C-cap (C0)[a]	C-cap-Mut5 (C1)
ΔG_0 (kcal/mol)	9.2±0.4[b]	4.3±0.2	12.9±0.4	7.7±0.4
m (kcal/mol/M)	1.34±0.04	1.03±0.06	0.53±0.04	0.70±0.03
J[c] (kcal/mol)		−15.2±0.4		

[a] Original C-cap, as present in NI_2C and NI_3C.
[b] All the errors reported are standard deviations (see Materials and Methods).
[c] Coupling parameter.

systematically increased in size. This knowledge also has practical consequences, as it will influence the design of libraries of repeat proteins for applications.[5,18] For AR proteins, individual repeats are not structurally stable,[19] and the favorable contributions to the overall fold are entirely due to the interaction between neighboring repeats. It becomes thus of interest to study this effect quantitatively.

To simplify the analysis, we used full-consensus repeat proteins with identical sequence, having a different number of repeats, and with two different C-capping repeats. The original C-cap had previously been identified as the least stable repeat within the protein,[7] and its replacement by a designed C-cap stabilizes the whole protein. The challenge with full-consensus repeat proteins is that their resonances in NMR are significantly more difficult to assign due to the repetitive nature of the sequence. Nevertheless, we could demonstrate that full backbone assignments are possible using a suitable set of 3D triple-resonance experiments in combination with PRE data. This allowed us to use a variety of NMR experiments to characterize the denaturation behavior at residue resolution, such as $^{1}H/^{2}H$ exchange over many orders of magnitude and the measurement of chemical shift and heteronuclear NOE as a function of denaturant.

Stability-determining role of the C-cap

We confirmed by direct NMR measurements that the wild-type C-cap is significantly less stable than the designed Mut5 C-cap. This had previously been deduced from MD calculations and indirectly from global unfolding experiments, and the design of the new C-cap was also inspired by MD calculations.[7] Here, we not only confirmed the relatively low stability of the original C-cap (taken from a natural ankyrin[6]) but also observe that there is a minor population of a second conformation both at the C terminus in NI_2C and NI_3C, encompassing the last five residues of the protein in a largely unfolded state, with the flexibility being proven by the $^{15}N\{^{1}H\}$-NOE data. Since two sets of resonances are observed, the interconversion between the two forms must be slow on the NMR time scale (slower than 4 ms). This puts an upper limit on the interconversion rate, such that the lifetime of both conformations is significantly longer than required for simple helix–coil transitions that can be as fast as 100 ns, indicating that additional interactions must be formed during the transition.

The original C-cap has frequently shown higher *B*-factors in crystal structures, and it is this region that is least well superimposed between different DARPin structures. In summary, it appears that this original C-cap, which was derived from a natural ankyrin, is not optimally packed against the central repeats. In contrast, the newly designed Mut5 C-cap does not display a second set of resonances. It also shows no evidence of selective early loss of C-cap cross-peaks in GdmCl titrations, its $^{1}H/^{2}H$ exchange rates are at least as slow as those of the N-cap, and the crystal structure is characterized by a better packing against the internal repeats (Kramer *et al.*, submitted). We have now direct evidence for the energetic consequences of this coupling, since the native-state hydrogen exchange is indeed significantly slower in the internal repeats of NI_3C_Mut5 than in NI_3C (Fig. 5).

Coupling of adjacent repeats largely influences the folding energy landscape

The increase in stability of repeat proteins with the number of repeats has been observed for ARs, armadillo repeats, and tetratricopeptide repeats.[11,12] One of the relatively simple quantifications to explain these relations is an Ising-type model.[10–12] In this model, each individual repeat is treated as an autonomous unit that is only coupled to its neighbors. For successful *in vivo* folding, special capping repeats with a hydrophilic surface are required, which are of lower intrinsic stability than the internal ones (this is true also for the newly designed Mut5 C-cap). The expectation from the Ising-type model is that the stability of repeats depends on their position in the protein: the most central ones would be expected to be more stable than those closer to the caps, because the central ones have a lower probability of having an unfolded neighbor. This effect is further enhanced by the lower intrinsic stability of the capping repeats. In particular, the central repeat of a NI_3C molecule should be the most stable.

The NMR methods used here have allowed us now to investigate the stability of the individual repeats directly. In native buffer, $^{1}H/^{2}H$ exchange rates were found to be very similar for corresponding positions in the different repeats, and the central internal repeat does not exhibit significantly higher PFs. Expectations of PFs using the Ising model parameterized here are depicted in Fig. 10. These calculations predict that PFs for the internal repeats are higher than those of the capping repeats, as is found experimentally. However, the PFs of the internal repeats are lower than predicted from the model and do not show the expected highest PF for the central repeat. This is most probably due to local fluctuations, which can formally be seen as an exchange from the native state. The computed $\Delta G_{(HX)}$ values of NI_3C and NI_3C_Mut5 are thus smaller than those from the GdmCl-denaturation experiments measured by CD,[7,8] and hence, in native buffer, local fluctuations must significantly contribute to $^{1}H/^{2}H$ exchange. Thus, local fluctuations not only equalize the observed exchange rates of the internal repeats but

also make them faster than the values expected from repeat unfolding.

H/D exchange directly from the native state has been proposed for the consensus tetratricopeptide repeat (CTPR)[15] to accommodate deviations from expectations of the Ising model. However, this is difficult to distinguish from local fluctuations. The differences between measured and H/D exchange rates expected from the Ising model in the full-consensus DARPins are much greater than the differences found in CTPR, possibly due to the much higher overall stabilities of the DARPins, leading to an extremely rare complete unfolding of single repeats. There may be an intrinsic occurrence of small fluctuations that limits the maximal PF.

The discrepancy of ΔG values for global unfolding as determined from the CD measurements in the presence of denaturant and those computed from the measured exchange rates of the most slowly exchanging residues thus indicates that these exchange events are not triggered by global unfolding. The protein NI_3 that lacks the C-cap displays a good-quality [^{15}N,^{1}H]-HSQC spectrum with signal dispersion similar to NI_3C (Fig. S15). However, the protein tends to precipitate over days at 310 K and its amide proton exchange is accelerated. Nevertheless, this well-dispersed spectrum demonstrates that species in which single repeats are unfolded are still stable for short periods of time and may thus be intermediates in larger local unfolding and refolding events. Such subpopulations of NI_3C or NI_3C_Mut5 can either refold or continue unfolding. The higher intrinsic stability of the Mut5 C-cap increases its probability for refolding over that of the wild-type C-cap. In addition, the better coupling of the new C-cap to I-3 reduces local exchange in the internal repeats in NI_3C_Mut5 compared to NI_3C and propagates the stability increase through the rest of the molecule.

In the presence of high concentrations of GdmCl (e.g., 3.5–4.0 M), exchange rates of NI_3C_Mut5 are strongly accelerated, and differences in exchange rates now become clearly visible between the amide protons of the I-1 or I-3 and the I-2 repeats (Fig. 10d). After approximately 4 weeks of exchange at 310 K in 4 M GdmCl, only peaks from signals of the central repeat remain for NI_3C_Mut5 (Fig. 8). At 3.5 M GdmCl, rates of residues within I-2 are slower than those of residues within I-1 and I-3, with the fastest rates being observed for I-1 (Fig. 9). Conversely, at higher temperatures in the absence of denaturant, exchange is faster, but the difference between the internal repeats remains very small. This suggests that when the whole protein is destabilized enough by denaturant, ^{1}H/^{2}H exchange by global unfolding of one repeat eventually becomes faster than exchange by local fluctuations, and the differences expected from the Ising-type model are indeed observed. In other words, the native DARPins are so stable and unfold so slowly in native buffer that local fluctuations put an upper limit to the residence time of a proton. However, under conditions of increased denaturant concentrations, partially unfolded species do not predominantly refold but rather continue unfolding such that under these conditions the exchange rates at least potentially report on unfolding of individual repeats.

The measurements of exchange in 3.5 M GdmCl are consistent with the staircase appearance expected from the predictions based on the Ising model (cf., Figs. 9c and 10d). We noticed, however, that the differences between exchange rates of I-1, I-2, and I-3 in the presence of denaturant are still smaller than those predicted based on an Ising model, which has been parameterized from optical spectroscopy to monitor unfolding and PF data for the capping repeats in buffer solution from the present work (Fig. 10). This discrepancy is most likely due to the fact that even under destabilizing conditions local fluctuations still significantly contribute to ^{1}H/^{2}H exchange. However, in contrast to the measurements at 310 K in native buffer (Fig. 9a), local fluctuations do not completely dominate exchange so that differences in stability become experimentally accessible (Fig. 9c).

Interestingly, the disappearance of signal dispersion in the [^{15}N,^{1}H]-HSQC spectra upon adding denaturant occurs well below the transition observed in the CD measurements. We have interpreted the collapse of signal dispersion as due to local fluctuations resulting in reduced packing of side chains that, however, does not lead to overall removal of tertiary structure. In fact, it may be a hallmark of the electrostatic nature of the inter-repeat interactions that they persist even if side-chain packing is loosened due to the less steep distance dependence in comparison to other types of interactions (e.g., van der Waals interactions or hydrogen bonds).

The slow H/D exchange rates in Figs. 9c and 10d were collected at 310 K while the data used to fit the Ising model were measured at 293 K.[8] A possible temperature dependence of stability may thus introduce some additional changes, which are not taken into account by the procedure used here to translate exchange rates from 310 to 293 K.[16] For example, a different dependence rate of stability loss of the N- and C-cap on temperature would also affect the adjacent repeats, whose stability depends on the adjacent cap being folded and could thus introduce a difference between repeats I-1 and I-3. Furthermore, at elevated temperature or in the presence of GdmCl as denaturant, the electrostatic interactions that mutually stabilize the neighboring repeats are reduced in strength. In either case, differences in stability become visible because unfolding of entire repeats starts to contribute to the observed exchange.

Nevertheless, even under destabilizing conditions, local exchange therefore continues to contribute to an extent that mostly levels out the differences between the repeats.

The Ising models[10–12] that have been proposed represent a coupled system of independent two-state folders, corresponding to the repeats. Whether the inherent assumption, namely, that the individual repeats unfold themselves cooperatively, is valid or not cannot easily be judged based on our data. More complicated models, involving partially denatured states of individual repeats, where, for example, only one of the helices is unfolded allowing accelerated $^{1}H/^{2}H$ exchange, would certainly also be compatible with our measurements. Different architectures of repeat proteins may differ in this respect, due to the intrinsic stability of the repeats and the strength of coupling.

Stabilizing features of the DARPins

Our NMR analysis has now allowed pinpointing structural features in the DARPins that are particularly important for stability. This will be valuable for the future development of new variants and additional libraries.

Significantly reduced exchange rates for amide protons are observed for the central positions of the helices (Fig. 6) in all proteins investigated in this work. In addition, selected positions within the long loops that connect the repeats are highly protected. Such high protection within loop regions is not necessarily expected. These protections highlight residues that are forming crucial interactions between repeats (*vide supra*)[7,20] and thereby significantly contribute to the coupling and the overall stability of the proteins.

We observed that the exchange rates are slower for residues of helix 1 compared to those of helix 2 of the same repeat module. We attribute this to the additional interactions helix 1 experiences with residues of the preceding repeat-connecting loop (especially through the conserved histidines of the TPLH motif). Moreover, the additional solvent shield provided by these loop residues may slow local unfolding events. Interestingly, this first helix is devoid of intrinsic helical propensity, as predicted by the program AGADIR[21] (Fig. S16), underlining the enormous importance of inter-repeat interactions for the stability of these proteins. This also implies that once such stabilizing interactions of the first helix are broken, the respective repeat is expected to unfold. Isolated modules have been shown to be largely unfolded.[19] Moderate helical propensities were computed only for the first helix of the N-cap, which has no preceding loop, and the second helix from each internal repeat.

Residues used for randomization in the DARPin library are mostly charged in the full-consensus DARPins, forming a tight network of attracting charges, involving loop residues as well as residues at the termini of the helices. This was postulated to generate additional interactions to make the full-consensus DARPins extraordinarily stable proteins.[7,20] The stabilizing interactions are formed by Asp and Lys residues from the loops and Arg and Glu residues in helix 1. It is therefore particularly interesting to note that around the charged loop residues, the largest ^{15}N chemical shift changes occur upon addition of GdmCl. Screening the favorable inter-repeat electrostatic interactions involving Asp and Lys residues in the loop may therefore be an important factor in denaturant-induced protein unfolding of these proteins. Nonetheless, GdmCl can safely be expected[22] to predominantly act on the main chain and nonpolar groups, and indeed, NI_3C_Mut5 does not unfold in 6 M NaCl (data not shown).

The proposed importance of ionic interactions for the stability of these repeat proteins, especially the role of the histidines (*vide supra*), is further demonstrated by the fact that the proteins unfold at room temperature at pH 3.5. Spectra recorded at that pH display reduced signal dispersion, and most residues are characterized by negative $^{15}N\{^{1}H\}$-NOEs.

Comparison with other repeat proteins

Native-state HX studies have also been performed with natural repeat proteins, which are much less stable than the full-consensus DARPins. The tumor suppressor AR protein p16[23] displayed very fast exchange for most residues within the dead time of the HX experiment, and only six residues could be followed. Those rates are consistent with the $\Delta G°$ measured in urea unfolding equilibrium.[24] This demonstrates that the extraordinary stability of the DARPins is not due to a high intrinsic stability of the ankyrin fold *per se*, but rather a consequence of consensus engineering.

Partially folded species have also been characterized in two CTPR proteins by an extensive $^{1}H/^{2}H$ exchange study.[15] In CTPR proteins, the outermost helices have much lower probability to be folded than the central helices, and these results are also consistent with an Ising model, requiring, however, the additional assumption that hydrogen exchange can take place also in the folded state of the protein. This may be equivalent to local fluctuations. As the slowest exchange rates are still 10–100 times faster than those measured here (PF about 10^4–10^7 for CTPR3[25] *versus* 10^4–10^8 for NI_2C and NI_3C and 10^4–10^9 for NI_3C_Mut5), this suggests that local fluctuations are also a consequence of protein stability.

Conclusions

Hydrogen exchange data as well as the denaturant-induced unfolding studies conducted in this

work indicate that the stability of the full-consensus AR proteins is greatly dependent on the coupling between repeats, most dramatically demonstrated by the stability-enhancing cap mutations that are propagated throughout the whole protein. Denaturant-induced unfolding, followed by $^{1}H/^{2}H$ exchange, is consistent with an Ising-type description of equilibrium folding of NI_3C_Mut5, while native-state exchange seems to be significantly governed by local fluctuations to allow exchange when unfolding events are too slow in these extremely stable proteins. Extraordinarily slowly exchanging protons indicate a stable core structure in the DARPins, which combines hydrophobic shielding with favorable electrostatic interactions. Key interactions between the loops and the helices cause a mutual stabilization.

Materials and Methods

Protein biochemistry and production of spin-labeled proteins

The repeat proteins NI_2C, NI_3C, and NI_3C_Mut5 and the respective Cys mutants (see below) were expressed in the *Escherichia coli* strain M15 (Qiagen) in M9 minimal medium containing ^{15}N-NH_4Cl as the sole nitrogen source: 5 ml of overnight culture (LB medium, 100 mg/l ampicillin, and 25 mg/l kanamycin, 37 °C) was used to inoculate 1-l cultures (M9 medium, 1% glucose, 150 μM thiamine, 30 mg/ml ampicillin, and 25 mg/ml kanamycin, 37 °C). At OD_{600} (optical density at 600 nm) = 0.6 (6 to 8 h), the cultures were induced with 500 mM IPTG and further incubated for 4 h.

For expression of triple ($^{15}N/^{13}C/^{2}H$)-labeled proteins, *E. coli* cells were adapted to high levels of $^{2}H_2O$ by streaking cells on agar plates with increasing content of $^{2}H_2O$ (LB agar in 50%, 100% $^{2}H_2O$) prior to inoculation. A 5 ml overnight culture (LB medium in $^{2}H_2O$, 1% ^{13}C-glucose, 100 mg/l ampicillin, and 25 mg/l kanamycin, 37 °C, 20 h) was used to inoculate 500 ml cultures (M9 medium in $^{2}H_2O$, 0.5% ^{13}C-glucose, 15 mg/l ampicillin, and 13 mg/l kanamycin, 37 °C). Cultures were induced at OD_{600} = 0.6 (after 12–18 h) and further incubated for 4 h. Purification was performed as described previously.[6,8] To facilitate complete back exchange of amide protons, we included an additional unfolding and refolding step in the purification procedure of the deuterated proteins. After loading the cell lysate, a Ni-NTA column was equilibrated with GdmCl-containing running buffer (5.5 M GdmCl for the back exchange of NI_2C and 7 M GdmCl for the back exchange of NI_3C and NI_3C_Mut5). Proteins were then incubated in the respective GdmCl solution on the column for 2 h at 20 °C. Stepwise refolding was subsequently achieved by lowering the GdmCl content in 0. 5-M steps to 0 M GdmCl prior to elution of the proteins. The purity was checked by SDS-PAGE, and the correct molecular mass was verified by mass spectrometry {[^{15}N]-NI_2C (experimental, 14.55 kDa; theoretical, 14.56 kDa), [^{15}N]-NI_3C (experimental, 18.12 kDa; theoretical, 18.13 kDa), [^{15}N]-NI_3C_Mut5 (experimental, 18.39 kDa; theoretical, 18.40 kDa), [^{15}N,^{13}C,^{2}H]-NI_2C (experimental, 15.82 kDa; theoretical, 15.99 kDa), [^{15}N,^{13}C,^{2}H]-NI_3C (experimental, 19.73 kDa; theoretical, 19.93 kDa), [^{15}N,^{13}C,^{2}H]-NI_3C_Mut5 (experimental, 20.05 kDa; theoretical, 20.23 kDa)}. In the case of the $^{15}N/^{13}C/^{2}H$-labeled proteins, we calculated a degree of deuteration of 78.9% (NI_2C), 80.3% (NI_3C), and 82.7% (NI_3C_Mut5). Yields for the ^{15}N-labeled proteins from 1 l were 90 mg for NI_2C, 50 mg for NI_3C, and 91 mg for NI_3C_Mut5, and for the ^{15}N,^{13}C,^{2}H-labeled proteins, 16 mg for NI_2C, 26 mg for NI_3C, and 10 mg for NI_3C_Mut5.

Production of spin-labeled proteins

Cys residues for attaching spin labels were introduced at positions 28, 150, and 155 using the following primers:

D28Cfor: 5′-TTTTGGTCAGGACTGCGAAGTTCG-TATCC-3′
D28Crev: 5′-TTTATACGAACTTCGCAGTCCTGAC-CAGCACG-3′
F150Cfor: 5′-TTTGTAAGACCGCTTGCGACATCTC-CATCG-3′
F150Crev: 5′-TTTGATGGAGATGTCGCAAG-CGGTCTTACCG-3′
D155Cfor: 5′-TTTGACTTAGCGATCTGCAACGG-TAACGAGG-3′
D155Crev: 5′-TTTTCGTTACCGTTGCAGATCGC-TAAGTCGAACGG-3′

The cysteine mutants were generated by inverse PCR using the respective forward and reverse oligonucleotide from the original expression plasmid pSW_NI_2C, pSW_NI_3C, and pSW_NI_3C_Mut5, with Pfu Turbo polymerase (1 min at 95 °C; followed by 18 cycles of 30 s at 95 °C, 1 min at 55 °C, and 10 min 68 °C; followed by 5 min at 68 °C, standard Pfu Turbo buffer). The remaining vector was digested with DpnI for 3 h and purified, chemically competent *E. coli* XL1-Blue cells were transformed, and the plasmids were sequenced using standard techniques.

The cysteine mutants of NI_2C, NI_3C, and NI_3C_Mut5 were incubated with 500 mM dithiothreitol (DTT) in PBS_{150} (50 mM phosphate and 150 mM NaCl, pH 7.4) for 30 min to ensure reduction of any intermolecular disulfide bridges. DTT was removed on a PD-10 column (Amersham) in PBS_{150} and the protein was immediately labeled at pH 6.4 under N_2 protection with MTSL (Toronto Research Chemicals) by adding MTSL spin label (stock solution 100 mM in dimethyl sulfoxide) to a final concentration of 3.8 mM to 800 μM protein. The reaction was allowed to proceed for 4 h at room temperature in the dark.[26,27] Excess MTSL was removed on a PD-10 column in PBS_{150}, and the labeled protein was concentrated using Amicon concentrator tubes. The success of the labeling reaction was verified by SDS-PAGE and mass spectrometry, where the peak from the spin-labeled protein complexes (SL) was the predominant one and unlabeled protein was a very minor species (<5%) {[^{15}N]-NI_2C-D28C-SL (experimental, 14.72 kDa; theoretical, 14.73 kDa), ^{15}N-NI_3C-D28C-SL (experimental, 18.29 kDa; theoretical, 18.30 kDa), ^{15}N-NI_3C-F150C-SL (experimental, 18.26 kDa; theoretical, 18.27 kDa), ^{15}N-NI_3C_Mut5-D28C-SL (experimental, 18.56 kDa; theoretical, 18.57 kDa), ^{15}N-NI_3C_Mut5-D155C-SL (experimental, 18.56 kDa; theoretical, 18.57 kDa)}.

Spin-label experiments

In order to identify residues in proximity to the spin label, we recorded 2D [1H,15N]-HSQC spectra of the Cys mutants for both the spin-labeled and non-spin-labeled species with 150–200 μM protein. Disulfide bond formation in the latter was suppressed by addition of 300 mM DTT. Cross-peaks were integrated in both spectra and their intensity ratio was calculated.

The respective Cys mutant was expressed in non-labeled medium (LB) and coupled to MTSL in order to exclude intermolecular "bleaching" effects. This species was mixed with ^{15}N-labeled Cys mutant protected with MalNEt to avoid dimer formation. For MalNEt coupling, the cysteine mutants of NI_2C, NI_3C, and NI_3C_Mut5 were incubated in 500 mM DTT in PBS_{150} (50 mM phosphate and 150 mM NaCl, pH 7.4) for 30 min to ensure disruption of all disulfide bridges. DTT was removed on a PD-10 column (Amersham) in PBS_{150} and the protein was immediately labeled with MalNEt (Fluka) in PBS_{150} at pH 7 under N_2 protection. A 10-fold molar excess of freshly prepared MalNEt in water was added, and the reaction was allowed to proceed for 2 h at room temperature. Excess MalNEt was removed on a PD-10 column in PBS_{150}, and the labeled protein was concentrated. Successful MalNEt labeling was verified by SDS-PAGE and mass spectrometry [NI_3C-D28C-MalNEt (experimental, 18.23 kDa; theoretical, 18.24 kDa), ^{15}N-NI_3C-F150C-MalNEt (experimental, 18.20 kDa; theoretical, 18.21 kDa), ^{15}N-NI_3C_Mut5-D28C-MalNEt (experimental, 18.50 kDa; theoretical, 18.51 kDa), ^{15}N-NI_3C_Mut5-D155C-MalNEt (experimental, 18.50 kDa; theoretical, 18.51 kDa)]. Both proteins were mixed in a 1:2 (^{15}N-MalNEt:^{14}N-SL) ratio. The ratio of peak integrals from spectra of this mixture and a reference sample of ^{15}N-MalNEt without ^{14}N-SL at the same protein concentration was evaluated.

NMR spectroscopy and data evaluation

NMR experiments were recorded using 700 μM solutions of NI_2C, NI_3C, or NI_3C_Mut5 in 50 mM phosphate buffer and 150 mM NaCl, pH 7.4. All NMR experiments were recorded at 310 K on Bruker Avance 600 or 700 MHz spectrometers equipped with cryoprobes. To avoid severe loss of sensitivity and prohibitively long pulse durations, we measured samples with high content of GdmCl in 3 mm NMR tubes. For backbone assignment, an approximately 79% deuterated, uniformly ^{13}C,^{15}N-labeled sample was used. All NMR experiments used pulsed-field gradients, sensitivity-enhancement schemes, and water suppression through coherence selection.[28,29] Deuterium decoupling was applied during relevant ^{15}N or ^{13}C evolution periods or delays. Experiments were selected from the Bruker standard pulse sequence library (with the sole exception of the MEXICO experiment). HNCACB/HN(CO)CACB spectra[30] and HN(COCACB)CG/HN(CACB)CG spectra[31] were used to link sequential amide groups via matching pairs of C^{α}/C^{β} and C^{γ} resonances. In addition, spin systems were linked via common carbonyl resonances using HNCO and HN(CA)CO experiments.[32] The usage of the HN(CACO)NH[33] experiment that provided direct correlations of amide groups with sequential nitrogen resonances proved to be particularly useful during assignment of the proton–nitrogen correlation map. A proton-detected version of the steady-state ^{15}N{^{1}H} heteronuclear nuclear Overhauser effect sequence was used for measurement of the heteronuclear NOE.[34]

All spectra were processed in TOPSPIN using mirror-image linear prediction for constant-time evolution periods. Spectra were mainly analyzed in the program CARA,[35] while batch processing of exchange spectra was accomplished with the programs XEASY[36] and SPSCAN.

Measurement of amide proton exchange

Slow amide proton exchange was measured by deuterium exchange experiments conducted at both 310 and 290 K. The ^{15}N-labeled proteins were lyophilized from the native buffer. To start the ^{1}H/^{2}H exchange reaction, we dissolved the proteins in 99.9% ^2H_2O to yield concentrations of 750 μM, and a first HSQC spectrum was acquired 5 min thereafter. Further 28 time points were taken over 24 h at 290 K. In a second set of experiments, deuterium exchange was monitored over a period of 5 to 12 months at 310 K. These slow proton–deuterium exchange rates were measured using standard [^{15}N,^{1}H]-HSQC experiments. Finally, ^{1}H,^{2}H exchange in native buffer at 333 K (60 °C) was measured for NI_3C_Mut5 by incubating the sample at 333 K in a water bath over the time span of 28 days, interrupted by short 1.5 h measurements at 310 K (at this temperature to facilitate peak identification). Since exchange in native buffer is extremely slow at 310 K for residues of the internal repeats, the introduced error in the kinetics by measuring at 310 K instead of 333 K is negligible.

Faster exchange rates were derived from a series of MEXICO experiments.[13] The pulse sequence used contained doubly matched ^{13}C and ^{15}N filters. Moreover, to avoid the devastating effects of radiation damping on cryoprobes at 700 MHz, a weak gradient was continuously applied during the recovery delay.

H/D exchange rates in the presence of 1 or 2 M GdmCl (NI_3C) or 3.5 and 4.0 M GdmCl (NI_3C_Mut5) were measured at 310 K by dissolving the lyophilized protein in fully deuterated GdmCl buffer of the corresponding GdmCl concentration. Up to 20 time points were taken over a period of 6 to 8 weeks.

For data collected at 290 K, the assignment (obtained at 310 K) was transferred to 290 K by a series of 2D [^{15}N,^{1}H]-HSQC spectra recorded in 2 K steps between 290 and 310 K.

Data analysis of amide proton exchange

Mono-exponential functions were fitted to the peak volumes of signals in the proton–deuterium exchange experiments using the Marquardt–Levenberg algorithm:

$$I(t) = I_0 \cdot e^{-k \cdot t} + I_{inf} \quad (1)$$

Similarly, the following function was fitted to the peak volumes from the MEXICO experiments

$$\frac{I}{I_{\mathrm{ref}}} = \frac{k}{-R_{\mathrm{w}} + R_1 + k} \cdot \left(e^{-R_{\mathrm{w}} t} - e^{-(R_1 + k)t} \right) \quad (2)$$

where R_{w} denotes the T_1 of water (determined in a separate experiment), R_1 is the rate constant for the decay of longitudinal amide proton magnetization, and k is the rate

constant for the exchange process of interest. Note that this function is slightly different from the one suggested by Hofmann *et al.*[37] to take into account the different treatment of water magnetization during the recovery delay necessary when recording data on cryoprobes.

PFs were calculated as the ratio k_{ch}/k_{exp}, where k_{exp} is the measured exchange rate and k_{ch} is the exchange rate of the amide in the unfolded state based on peptide models (dependent on temperature, pH, and neighboring amino acids).[9] The stabilizing free energy of the protecting structure can then be calculated as

$$\Delta G_{(HX)} = -RT\ln(k_{ex}/k_{ch}) \quad (3)$$

Exchange rates determined at 290 K were converted to the expected values at 310 K according to

$$k_{ex}(T) = k_{ex}(290)e^{-\frac{E_a}{R}\left(\frac{1}{T}-\frac{1}{290}\right)} \quad (4)$$

where E_a=19 kcal/mol and R=1.986 cal/mol·K is the gas constant,[16] and the data recorded at 333 K were treated in an analogous fashion.

Measurement of GdmCl- or pH-induced equilibrium unfolding by NMR

For measuring HSQC spectra in GdmCl, the samples were equilibrated at the corresponding GdmCl concentration overnight at 20 °C. The final GdmCl concentrations were determined by the refractive index. Because of the high salt content and signal broadening, spectra were recorded with increasing numbers of scans with increasing GdmCl concentrations. The assignment was transferred stepwise from 0 to 3.6 M (NI_3C) and 5 M (NI_3C_Mut5) denaturant. The differences in ^1H and ^{15}N chemical shifts between 0 and 3.6 or 5 M denaturant for selected residues were plotted against the protein sequence.

For measurements of the proteins at pH 3.5, a different buffer (7.5 mM phosphate, 7.5 mM citric acid and 7.5 mM boric acid, 85 mM KCl) was prepared. The pH was quickly lowered from 7.4 to 3.5 by adding 20 ml of this pH 3.5 buffer to 50 μl of the protein in PBS_{150} buffer. The solution was concentrated by centrifugation and re-diluted 4 times with this buffer in order to completely exchange the buffer. The first measurement was started approximately 2 h after the initial mixing of buffers.

Fit to Ising model

The Ising model presented in Ref. 8 was extended to take into account the difference in stability observed between the N-cap and the original as well as the mutated C-caps by introducing separate sets of stability parameters for each of them, in addition to the set describing the internal repeats. The functional form for the effective conformational free energy is:

$$\Delta G_{Conf}(\{s_i\};D,L,y) = \Delta G^I(D)\sum_{i=2}^{L-1} s_i + \Delta G^N(D)\cdot s_1 + \Delta G^y(D)\cdot s_L + J\sum_{i=1}^{L-1} s_i s_{i+1} \quad (5)$$

where s_i is a variable describing the state of the ith repeat (1 when folded, 0 when unfolded), L is the total number of repeats in the protein, D is the denaturant concentration, and y indicates the type of C-cap of the protein (C0 for the original C-cap or C1 for the mutated C-cap). The $\Delta G^x(D) = \Delta G_0^x + m^x \cdot D$ are the stabilities of the repeat of type x (with x=I, N, C0, C1 for the internal, N-cap, original C-cap, and mutated C-cap repeat, respectively) and depend linearly on the denaturant concentration. Thus, the model is characterized by nine free parameters, that is, the coupling parameter J and 4×2 stability parameters (ΔG_0^I, ΔG_0^{C0}, ΔG_0^{C1}, m^I, m^N, m^{C0}, and m^{C1}) instead of the previously used five parameters in Ref. 8. To avoid overfitting, we globally fitted the model to a large set of data, comprising the CD-monitored equilibrium unfolding data[7,8] and the PF values for the caps in the absence of denaturant reported in the present work. The PF values for the internal repeats have been excluded from the fit, as they are affected by local fluctuations. The fit to the CD data was obtained following the procedure described in Ref. 8. The fit of the PF data was obtained by assuming that the largest PF of repeat i is inversely proportional to the probability of observing the repeat unfolded, p_u,[15]

$$PF(D,i,L) \approx \frac{1}{p_u(D,i,L)} \quad (6)$$

with

$$p_u(D,i,L) = 1 - \sum_{\{s_j\}} P_L(\{s_j\};D)\cdot s_i \quad (7)$$

where $P_L(\{s_j\};D)$ is the probability of observing the conformation $\{s_j\}$ [see Eq. (19) in Ref. 8] and the sum is extended to all possible conformations. The global fit was obtained by minimizing the χ^2, which had a contribution from the PF and one from the CD data, weighted so that both sets of data contribute similarly. χ^2 was minimized using the Levenberg–Marquardt procedure and the errors reported on the parameters are standard deviations obtained from the inverse of the approximate Hessian matrix of the χ^2.

All amide proton, ^{15}N, C^α, and C^β chemical shifts of NI_2C, NI_3C, and NI_3C_Mut5 have been deposited in the Biological Magnetic Resonance Data Bank database under accession codes 16718, 16717, and 16716, respectively.

Acknowledgements

The authors thank Dr. Annemarie Honegger for software predicting the distance dependence of spin labels and Dr. Jiri Mares for writing scripts for the calculation of rate constants. This work was supported by Swiss National Science Foundation grant no. CRSI00_122686 (to O.Z.) and the NCCR Structural Biology (to A.P.).

Supplementary Data

Supplementary data associated with this article can be found, in the online version, at doi:10.1016/j.jmb.2010.07.031

References

1. Andrade, M. A., Perez-Iratxeta, C. & Ponting, C. P. (2001). Protein repeats: structures, functions, and evolution. *J. Struct. Biol.* **134**, 117–131.
2. Marcotte, E. M., Pellegrini, M., Yeates, T. O. & Eisenberg, D. (1999). A census of protein repeats. *J. Mol. Biol.* **293**, 151–160.
3. Kobe, B. & Kajava, A. V. (2000). When protein folding is simplified to protein coiling: the continuum of solenoid protein structures. *Trends Biochem. Sci.* **25**, 509–515.
4. Sedgwick, S. G. & Smerdon, S. J. (1999). The ankyrin repeat: a diversity of interactions on a common structural framework. *Trends Biochem. Sci.* **24**, 311–316.
5. Binz, H. K., Amstutz, P., Kohl, A., Stumpp, M. T., Briand, C., Forrer, P. *et al.* (2004). High-affinity binders selected from designed ankyrin repeat protein libraries. *Nat. Biotechnol.* **22**, 575–582.
6. Binz, H. K., Stumpp, M. T., Forrer, P., Amstutz, P. & Plückthun, A. (2003). Designing repeat proteins: well-expressed, soluble and stable proteins from combinatorial libraries of consensus ankyrin repeat proteins. *J. Mol. Biol.* **332**, 489–503.
7. Interlandi, G., Wetzel, S. K., Settanni, G., Plückthun, A. & Caflisch, A. (2008). Characterization and further stabilization of designed ankyrin repeat proteins by combining molecular dynamics simulations and experiments. *J. Mol. Biol.* **375**, 837–854.
8. Wetzel, S. K., Settanni, G., Kenig, M., Binz, H. K. & Plückthun, A. (2008). Folding and unfolding mechanism of highly stable full-consensus ankyrin repeat proteins. *J. Mol. Biol.* **376**, 241–257.
9. Krishna, M. M., Hoang, L., Lin, Y. & Englander, S. W. (2004). Hydrogen exchange methods to study protein folding. *Methods*, **34**, 51–64.
10. Zimm, B. H. & Bragg, J. K. (1959). Theory of the phase transition between helix and random coil polypeptide chains. *J. Chem. Phys.* **31**, 526–535.
11. Mello, C. C. & Barrick, D. (2004). An experimentally determined protein folding energy landscape. *Proc. Natl Acad. Sci. USA*, **101**, 14102–14107.
12. Kajander, T., Cortajarena, A. L., Main, E. R., Mochrie, S. G. & Regan, L. (2005). A new folding paradigm for repeat proteins. *J. Am. Chem. Soc.* **127**, 10188–10190.
13. Gemmecker, G., Jahnke, W. & Kessler, H. (1993). Measurements of fast proton-exchange rates in isotopically labeled compounds. *J. Am. Chem. Soc.* **115**, 11620–11621.
14. Palmer, A. G. (2004). NMR characterization of the dynamics of biomacromolecules. *Chem. Rev.* **104**, 3623–3640.
15. Cortajarena, A. L., Mochrie, S. G. & Regan, L. (2008). Mapping the energy landscape of repeat proteins using NMR-detected hydrogen exchange. *J. Mol. Biol.* **379**, 617–626.
16. Bai, Y., Milne, J. S., Mayne, L. & Englander, S. W. (1993). Primary structure effects on peptide group hydrogen exchange. *Proteins*, **17**, 75–86.
17. Kohl, A., Binz, H. K., Forrer, P., Stumpp, M. T., Plückthun, A. & Grütter, M. G. (2003). Designed to be stable: crystal structure of a consensus ankyrin repeat protein. *Proc. Natl Acad. Sci. USA*, **100**, 1700–1705.
18. Parmeggiani, F., Pellarin, R., Larsen, A. P., Varadamsetty, G., Stumpp, M. T., Zerbe, O. *et al.* (2008). Designed armadillo repeat proteins as general peptide-binding scaffolds: consensus design and computational optimization of the hydrophobic core. *J. Mol. Biol.* **376**, 1282–1304.
19. Mosavi, L. K., Minor, D. L. J. & Peng, Z. Y. (2002). Consensus-derived structural determinants of the ankyrin repeat motif. *Proc. Natl Acad. Sci. USA*, **99**, 16029–16034.
20. Merz, T., Wetzel, S. K., Firbank, S., Plückthun, A., Grütter, M. G. & Mittl, P. R. (2008). Stabilizing ionic interactions in a full-consensus ankyrin repeat protein. *J. Mol. Biol.* **376**, 232–240.
21. Munoz, V. & Serrano, L. (1994). Elucidating the folding problem of helical peptides using empirical parameters. *Nat. Struct. Biol.* **1**, 399–409.
22. Pace, C. N. & Shaw, K. L. (2000). Linear extrapolation method of analyzing solvent denaturation curves. *Proteins*, 1–7.
23. Tang, K. S., Fersht, A. R. & Itzhaki, L. S. (2003). Sequential unfolding of ankyrin repeats in tumor suppressor p16. *Structure*, **11**, 67–73.
24. Boice, J. A. & Fairman, R. (1996). Structural characterization of the tumor suppressor p16, an ankyrin-like repeat protein. *Protein Sci.* **5**, 1776–1784.
25. Main, E. R., Stott, K., Jackson, S. E. & Regan, L. (2005). Local and long-range stability in tandemly arrayed tetratricopeptide repeats. *Proc. Natl Acad. Sci. USA*, **102**, 5721–5726.
26. Lietzow, M. A., Jamin, M., Dyson, H. J. & Wright, P. E. (2002). Mapping long-range contacts in a highly unfolded protein. *J. Mol. Biol.* **322**, 655–662.
27. Hornung, T., Volkov, O. A., Zaida, T. M., Delannoy, S., Wise, J. G. & Vogel, P. D. (2008). Structure of the cytosolic part of the subunit β-dimer of *Escherichia coli* F0F1-ATP synthase. *Biophys. J.* **94**, 5053–5064.
28. Kay, L. E., Keifer, P. & Saarien, T. (1992). Pure absorption gradient enhanced heteronuclear single-quantum correlation spectroscopy with improved sensitivity. *J. Am. Chem. Soc.* **114**, 10663–10665.
29. Keeler, J., Clowes, R. T., Davis, A. L. & Laue, E. D. (1994). Pulsed-field gradients: theory and practice. *Methods Enzymol.* **239**, 145–207.
30. Shan, X., Gardner, K. H., Muhandiram, D. R., Rao, N. S., Arrowsmith, C. H. & Kay, L. E. (1996). Assignment of N-15, C-13(alpha), C-13(beta), and HN resonances in an N-15, C-13, H-2 labeled 64 kDa trp repressor–operator complex using triple-resonance NMR spectroscopy and H-2-decoupling. *J. Am. Chem. Soc.* **118**, 6570–6579.
31. McCallum, S. A., Hitchens, T. K. & Rule, G. S. (1998). Unambiguous correlations of backbone amide and aliphatic gamma resonances in deuterated proteins. *J. Magn. Reson.* **134**, 350–354.
32. Yamazaki, T., Lee, W., Arrowsmith, C. H., Muhandiram, D. R. & Kay, L. E. (1994). A suite of triple-resonance NMR experiments for the backbone assignment of N-15,C-13,H2-labeled proteins with high sensitivity. *J. Am. Chem. Soc.* **116**, 11655–11666.
33. Weisemann, R., Rüterjans, H. & Bermel, W. (1993). 3D triple-resonance NMR techniques for the sequential assignment of NH and ^{15}N resonances in ^{15}N- and ^{13}C-labelled proteins. *J. Biomol. NMR*, **3**, 113–120.

34. Noggle, J. H. & Schirmer, R. E. (1971). *The Nuclear Overhauser Effect—Chemical Applications.* Academic Press, New York, NY.
35. Keller, R. (2004). *The Computer Aided Resonance Assignment.* CANTINA Verlag, Goldau, Switzerland.
36. Bartels, C., Xia, T. H., Billeter, M., Güntert, P. & Wüthrich, K. (1995). The program XEASY for computer-supported spectral analysis of biological macromolecules. *J. Biomol. NMR*, **6**, 1–10.
37. Hofmann, H., Weininger, U., Low, C., Golbik, R. P., Balbach, J. & Ulbrich-Hofmann, R. (2009). Fast amide proton exchange reveals close relation between native-state dynamics and unfolding kinetics. *J. Am. Chem. Soc.* **131**, 140–146.
38. Loftus, D., Gbenle, G. O., Kim, P. S. & Baldwin, R. L. (1986). Effects of denaturants on amide proton exchange rates: a test for structure in protein fragments and folding intermediates. *Biochemistry*, **25**, 1428–1436.